Physica A 505 (2018) 1127–1138

Contents lists available at ScienceDirect

Physica A

journal homepage: www.elsevier.com/locate/physa

Generalized AIC method based on higher-order moments and entropy of financial time series

Shiyun Xu, Menglin Shao, Wenxuan Qiao, Pengjian Shang *

Department of Mathematics, School of Science, Beijing Jiaotong University, Beijing 100044, PR China

HIGHLIGHTS

- We modify AIC method by extending variance to high-order statistics.
- We use information entropy to promote generalize AIC method ulteriorly.
- A new perspective of analyzing the fluctuation of financial time series which is named AIC plane, is proposed in order to derive more accurate results.
- There are some interesting results of stock markets in different areas when using generalized AIC method.

ARTICLE INFO

Article history:
Received 1 January 2018
Received in revised form 27 February 2018
Available online 13 April 2018

Keywords:
AIC method
Skewness
Kurtosis
Entropy
Financial time series

ABSTRACT

In this paper, a generalized method of traditional Akaike information criterion is proposed as a new measurement to compare and evaluate the volatility behaviors of time series in stock market. This new method is modified by extending variance to high-order statistics such as skewness, kurtosis, and permutation entropy, so as to demonstrate the different aspects of volatility behaviors of time series compared to low-order method. Furthermore, a new model of creating an AIC plane is proposed in order to derive more accurate results. Numerical simulations are conducted over synthetic data to provide comparative study. In addition, further reports about the results of distinguishing behaviors in stock market composite index of America, China and Hong Kong by using generalized AIC method and AIC plane are utilized to reflect the feasibility. Our results can effectively differentiate multiscale volatility details of time series from three areas.

1. Introduction

Sequences in complex systems, represented by financial markets, generally exhibit fluctuations on a wide range of time scales that depends on data [1–3], and its dynamical behaviors of the economic index are consistent with the underlying economic trends [4–13]. Various statistical techniques, models and theoretical methods have been introduced to characterize volatility in financial time series from different aspects, in order to reflect the features of the dynamics of financial markets [3,5,14–32].

The Akaike information criterion (AIC) is used primarily for estimating the quality of statistical model [33]. There is no doubt that increase the number of free parameters can improve the superiority of data fitting. While looking for models that can best interpret data but contain minimal free parameters, the AIC method encourages the benignity of data fitting but avoids Overfitting, which makes it better than other methods to some extent. Recently researches are trying to extend

* Corresponding author.
E-mail addresses: 15321023@bjtu.edu.cn (S. Xu), pjshang@bjtu.edu.cn (P. Shang).

https://doi.org/10.1016/j.physa.2018.04.048
0378-4371/

statistical models by replacing the variance to high-dimensional statistics so that the results will be more accurate because of the reduction of uncertainty during characterization process [34–40]. In addition, inspired by the AIC-Selector, which is a reliable tool for the automated detection of acoustic emission signal, researchers innovate to use AIC for the identification and assessment of defects in time-dependent series [41–43]. This method can be effective in selecting accurate models in the presents of outliers. In this article, we generalized the Akaike information criterion to high-order statistics such as skewness and kurtosis, so as to investigate the volatility details of financial time series in the case of higher order moments. Since entropy is a stability and robustness nonlinear measurement to characterize the complexity of a financial time series, and permutation entropy has been recently suggested as a novel measurement for nonlinear time series [44–49], we also try to modify AIC with permutation entropy. Moreover, inspired by the entropy plane [50,51], we creatively proposed a totally new method — AIC plane to demonstrate the volatility of financial time series with respect to nonlinear monotone transformations. By using logistic map and lozi map [52], we generate time series over synthetic and real data to simulate and inspect the consequence of our models.

The remainder of the paper is organized as follows. In Section 2, we describe the methodology of AIC, generalized AIC method, and AIC plane. Next, Section 3 presents the simulation of logistic map and lozi map. Section 4 outlines the database acquisition and preprocessing, and then presents the results of SAIC, KAIC and PEAIC that apply to real stock markets to analyze the volatility of time series. Finally, conclusion is demonstrated in Section 5.

2. Methodology

2.1. Generalized AIC method

AIC method has been used to estimating the quality of statistical model, since it optimizes a good trade-off between the complexity and the fitness of the model. In addition, it can be calculated directly from the signal itself [52]. According to the advantage shown above, this criterion has been used to determine the onset of seismic waves in seismology in combination with two autoregressive fits. On the basis of this assumption, an autoregressive-Akaike information criteria (AR-AIC) method has been used to detect P and/or S phases [53–55]. For the AR-AIC picker, the order of the AR process must be specified through trial and error, and the AR coefficients have to be calculated for both intervals. Compare to the AR-AIC picker, Maeda uses a different AIC picker [56], which can be calculated directly from the records itself without fitting them with the AR processes, and this direct AIC method defines an AIC value for each sample n of a signal:

$$AIC_n = n \cdot \ln\left(\sigma^2_{1,n}\right) + (N - n - 1) \cdot \ln\left(\sigma^2_{n+1,N}\right) \tag{1}$$

We utilize the method above to study financial time series of stock market. Moreover, in order to investigate the volatility scaling property of a complex dynamical system such as stock market in a new perspective, we extended the AIC method to higher moments and proposed new methods, namely SAIC method, KAIC method and PEAIC method.

The SAIC and KAIC procedure consists of four steps.

Step 1

Consider a stock time series $x = (x_1, x_2,\dots, x_N)$, and we use a sliding variable n to divide it into two parts, which are denoted as $x_{1,n}$ and $x_{n+1,N}$ respectively.

Step 2

For each n ranging from 1 to N-1, we calculate the skewness and the kurtosis of two sequences $x_{1,n}$ and $x_{n+1,N}$ respectively.

Step 3

We standardize the data to ensure the resulting are valid in the AIC formula:

$A\,(i,j)$ is the skewness (or kurtosis) of all the data from x_i to x_j. In order to make the $A\,(i,j)$ standard to facilitate the processing, they are converted into:

$$\widetilde{A}(i,j) = \left\{\frac{A(i,j) - minA(i,j)}{maxA(i,j) - minA(i,j)} + \frac{1}{N}\right\} \tag{2}$$

where N is the total number of our sample.

Step 4

By substituting what we got from step 2 into the generalized AIC equation as follows, we get $SAIC(n)$ and $KAIC(n)$ that take n as the independent variable:

$$SAIC\,(n) = n \times ln[\widetilde{A}_s\,(1,n)] + (N - n - 1) \times \ln[\widetilde{A}_s\,(n+1,N)] \tag{3}$$

$$KAIC\,(n) = n \times ln[\widetilde{A}_k\,(1,n)] + (N - n - 1) \times \ln[\widetilde{A}_k\,(n+1,N)] \tag{4}$$

where $\widetilde{A}_s\,(i,j)$ is the standard skewness, and $\widetilde{A}_k\,(i,j)$ is the standard kurtosis of all the data from x_i to x_j.

Besides, in view of the significant role of entropy when characterizing the complexity of a financial time series as a stability and robustness nonlinear measurement, we also try to modify AIC with permutation entropy, which is denoted as PEAIC.

The permutation entropy algorithm has shown a good application prospect in signal mutation detection for that it can effectively magnify the small change of the time series with simple calculation as well as high sensitivity.

The permutation entropy is defined as follows:

Consider a time series with N values: $(x_1, x_2, \ldots, x_N)$ according to their relative values, we organize the $N-1$ pairs of neighbors, finding k ($k \geq 0$) pairs for which $x_t < x_{t+1}$ and j ($j = N-k-1$) pairs for which $x_t > x_{t+1}$. So k of N-1 pairs of values are represented by the permutation 01 ($x_t < x_{t+1}$) and j of N-1 are represented by 10. We define the permutation entropy of order $n = 2$ as a measure of the probabilities of the permutations 01 and 10 [45]. So we get permutation entropy of the series when $n = 2$:

$$H(2) = -\left(\frac{k}{N-1}\right)\log\left(\frac{k}{N-1}\right) - \left(\frac{j}{N-1}\right)\log\left(\frac{j}{N-1}\right) \tag{5}$$

Here we give the methodology of PEAIC which consists of four steps.

Step 1

Consider a series $(x_1, x_2, \ldots, x_N)$, we divide them into two parts, which are denoted as $x_{1,n}$ and $x_{n+1,N}$ respectively.

Step 2

The first part has n values, where n ranging from 1 to N-1. Referring to the definition of permutation entropy of order 2, we get

$$H^1_{1,n} = -\left(\frac{k_1}{n-1}\right)\log\left(\frac{k_1}{n-1}\right) - \left(\frac{j_1}{n-1}\right)\log\left(\frac{j_1}{n-1}\right) \tag{6}$$

The other part has $N-n$ values. Analogously, by applying the method of permutation entropy to it, we get,

$$H^2_{n+1,N} = -\left(\frac{k_2}{N-n-1}\right)\log\left(\frac{k_2}{N-n-1}\right) - \left(\frac{j_2}{N-n-1}\right)\log\left(\frac{j_2}{N-n-1}\right) \tag{7}$$

Step 3

When sliding variable n changes from 1 to N-1, a matrix of $(N\text{-}1)\times 2$ dimension is got:

$$P = \begin{pmatrix} H^1_{1,1} & H^2_{2,N} \\ H^1_{1,2} & H^2_{3,N} \\ \cdots & \cdots \\ H^1_{1,N-1} & H^2_{N,N} \end{pmatrix}$$

Step 4

By substituting the matrix P that we get from step 3 into the PEAIC equation as follows:

$$PEAIC(n) = n \times \log(\widetilde{H}^1_{1,n}) + (N-n-1) \times \log(\widetilde{H}^2_{n+1,N}) \tag{8}$$

we get $PEAIC(n)$ that takes n ranging from 1 to N-1, where $\widetilde{H}^1_{1,n}$ and $\widetilde{H}^2_{n+1,N}$ are normalized permutation entropy.

2.2. The AIC plane

2.2.1. Tsallis entropy

Entropy has important applications in statistical mechanics and information theory. Over the past few decades, many problems of this concept have been discussed. Since the concepts of thermodynamic entropy which describe the nature of the success probability of a system were proposed, entropy has developed as a basic branch of modern science. Moreover, a large number of references begin to introduce different forms of entropies, such as Shannon entropy, Renyi entropy, Tsallis entropy and so on, which play indispensable roles in extended statistical mechanics.

Entropy shows the average amount of information. According to information theory, Shannon entropy is defined as:

$$H(A) = -\sum p(i)\log p(i) \tag{9}$$

In Eq. (9), $p(i)$ is the probability density distribution of a random variable.

Tsallis entropy is a generalized form of Shannon entropy which adds one more parameter. It is a measure of new information in statistical physics, and this new method can provide satisfactory physical explanation to those who have irregular shape pieces of hybrid or non-additive system. It is defined as follows:

$$S_q(A) = \frac{1}{q-1}\left(1 - \sum p(i)^q\right) \tag{10}$$

We standardize the daily stock index, denoting as $p(i)$.

Then we take $p(i)$ into following two formulas:

$$S_q^1(t) = \frac{1 - \sum_{i=0}^{n} \left(\frac{p(i)}{P_1(t)}\right)^q}{q-1} \tag{11}$$

$$S_q^2(t) = \frac{1 - \sum_{i=n+1}^{N} \left(\frac{p(i)}{P_2(t)}\right)^q}{q-1} \tag{12}$$

where $P_1(t)$ is:

$$P_1(t) = \sum_{i=0}^{t} p(i) \tag{13}$$

and $P_2(t)$ is:

$$P_2(t) = 1 - P_1(t) \tag{14}$$

The sum of entropy of two independent subsystems follows pseudo additivity:

$$S_q(t) = S_q^1(t) + S_q^2(t) + (1-q) \cdot S_q^1(t) \cdot S_q^2(t) \tag{15}$$

Similar to what we did in Section 2.1, we generalized AIC method with Tsallis entropy and put it into AIC plane.

2.2.2. AIC plane

Although PEAIC can reflect some fluctuation information that cannot be detected by traditional AIC method, the simultaneous equation model of PEAIC and SAIC or KAIC is not ideal as expected, which pushes us to find another entropy to construct a AIC plane.

Inspired by the permutation entropy plane [5,44], a new method, which we called AIC plane, is generated to demonstrate the volatility of financial time series. In this method, we creatively correlate three variables, denoted as SAIC, KAIC, Tsalis entropy, by setting two of them respectively as variable x and variable y, and the simulation shows that this measurement of volatility information in time series is effective. As AIC plane procedure is similar to generalized AIC method, so instead of giving more detailed description, we demonstrate more attention to its heuristic results.

3. Simulations of artificial time series

3.1. Logistic map model

Logistic map is a well-known polynomial mapping, and it is mathematically defined as:

$$x_{n+1} = rx_n(1 - x_n) \tag{16}$$

where r is a parameter and $0 < r < 4$, x_n ranges from 0 to 1.

3.1.1. Simulation of generalized AIC method

Utilizing the logistic map model, we construct time series $x = (x_1, x_2, \ldots, x_N)$. Here we keep the value of r in the range of $[3.7, 4.0]$ and step 0.1. For each value of r, we set an initial value $x_1 = 0.2$. Therefore, a time series will be obtained with the length of 452.

In Figs. 1–3, it is observed that for all values of r, curves of AIC almost have the same positive relationship with n. By contrast, In Fig. 2, curves of SAIC shows a strong fluctuation at first. Along with some slight wave, the curve declined gradually, which is opposite to curve AIC, and then, the larger parameter r is, the slower it decreases. In addition, we can find that curves of KAIC are more similar to curves of AIC, however the KAIC has more wispy waves than AIC. Furthermore, the falling wedge of KAIC comes later generally than curves of AIC. It is noteworthy that the curves of PEAIC in Fig. 4 is different from the other three when $r = 4.0$, and it has an obvious fluctuant decrease when $n = 90$.

Another fact that attract us is, comparing to the AIC curve, those three PEAIC curves fluctuate in the horizontal direction roughly as n increases, and there are small amplitude of high frequency fluctuations when $10 < n < 100$, and this undulation is weaker with the rise of n.

3.1.2. Simulation of AIC plane

In this section, we will keep parameter r in the range of $[3.7, 3.9]$ and step 0.1. And for each value of r, we still give x_1 an original value of 0.2. On this occasion, we will obtain three different logistic map series with the length of $n = 452$.

As shown in Fig. 5, the S-KAIC method can mark off three different time series effectively. As KAIC(n) goes up, the value of SAIC(n) declines at different velocity. Ignoring the difference of these three curves, it is noteworthy that small fluctuations with high frequency appear when KAIC and SAIC are not so big, which also means a small change in value of KAIC(n) gives

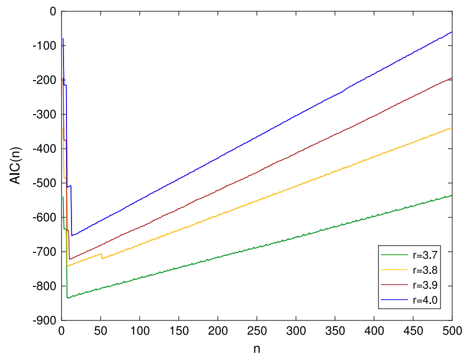

Fig. 1. Simulation of AIC based on logistic map.

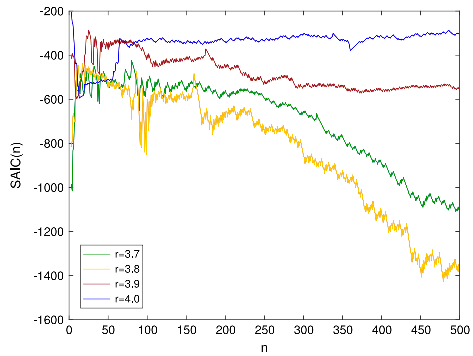

Fig. 2. Simulation of SAIC based on logistic map.

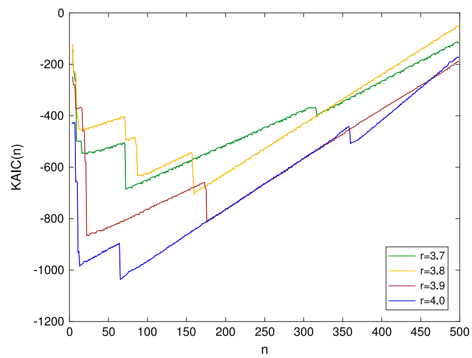

Fig. 3. Simulation of KAIC based on logistic map.

rise to a strong reaction of SAIC(n) comparatively. Then, the curve goes to a much smoother descending tendency as KAIC and SAIC are relatively large. This manifests a stationary relationship between the two generalized AIC methods.

Fig. 6 shows a relative size relationship of three curves of $r = 3.7$, $r = 3.8$, $r = 3.9$ which is similar to Fig. 5, but in a more legible way. What is different is that the curves consist of high frequency wavelet all the way, which means a subtle change of TEAIC(n) can cause relatively big change in SAIC(n). We can infer from Figs. 5 and 6 that SAIC is sensitive to KAIC and TEAIC to some extent.

According to Fig. 7, the K-TEAIC curve is a little bit different from the two curves above, so at the same level of TEAIC(n), the value of KAIC(n) when $r = 3.8$ is the largest, while the smallest value of KAIC(n) curve is corresponded to $r = 3.7$ and $r = 3.9$. In other words, the combination of KAIC and TEAIC reverses the relative size relationship of three time series. Furthermore, compared to Figs. 6 and 7, the curve of K-TEAIC is smoother, which embodies a relative insensitivity of KAIC and TEAIC.

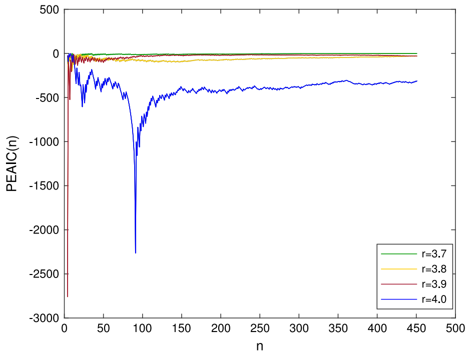

Fig. 4. Simulation of PEAIC based on logistic map.

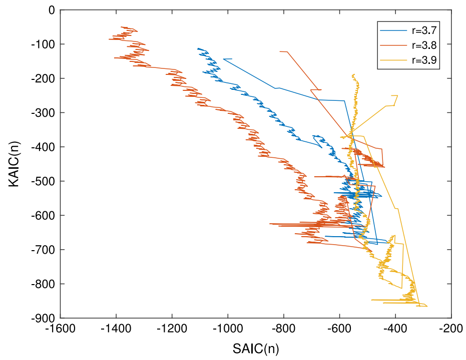

Fig. 5. Simulation of S-KAIC plane based on logistic map.

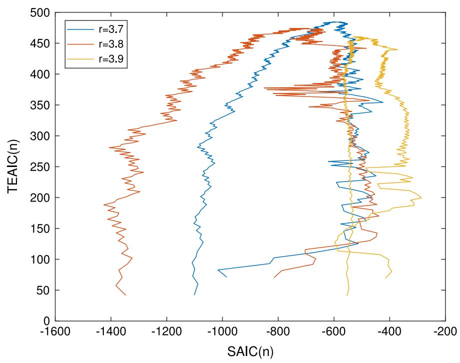

Fig. 6. Simulation of S-TEAIC plane based on logistic map.

3.2. Lozi map model

The Lozi map is a piecewise-linear variant of the H'enon map given by [52]:

$$x_{t+1} = 1 + y_n - ax_t \tag{17}$$

$$y_{t+1} = bx_t \tag{18}$$

in the chaotic regime ($a = 1.7$ and $b = 0.5$).

We can set $x_1 = 0.2, y_1 = 0.2$, therefore, we will obtain two different logistic map series with the length of $n = 452$.

Similarly, for all values of r, curves of AIC in Fig. 8 increase approximately the same trends as k changes. And the curves of SAIC in Fig. 9 decreased gradually, which is opposite to curve AIC. Besides, it can be easily observed that x decreases slower

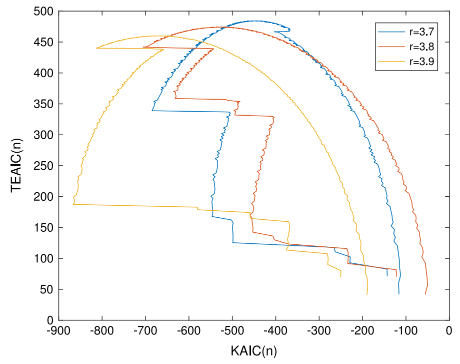

Fig. 7. Simulation of K-TEAIC plane based on logistic map.

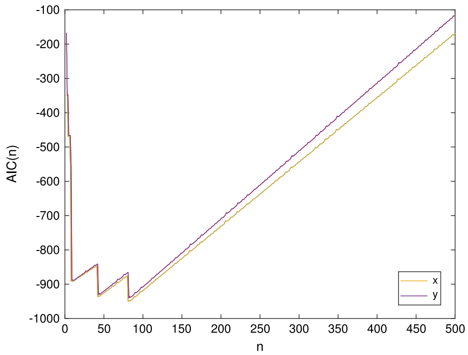

Fig. 8. Simulation of AIC based on Lozi map.

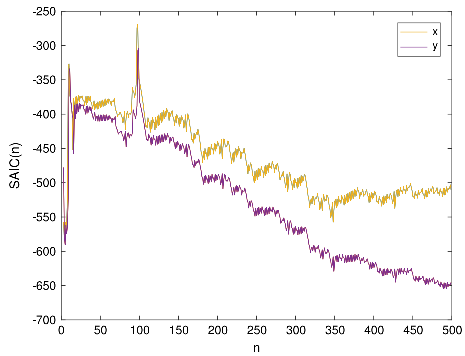

Fig. 9. Simulation of SAIC based on Lozi map.

than y, which means the value of x is always larger than y, and also in the case of KAIC. Compared with AIC, the KAIC in Fig. 10 declined more apparently when n is roughly between 60 to 100. Furthermore, it is distinct that for curves of AIC, y is bigger than x, but the curves of SAIC and KAIC demonstrates that x is bigger than y.

4. Numerical results of stock market

4.1. Stock data

For further discussing the AIC based on higher moments and entropy, we consider the series of stock market. We use three sets of data, namely, Shanghai securities composite index (SSEC), Hang Seng Index (HSI), and Dow Jones Index (DJI) from July 14, 2015 to July 14, 2017 from the yahoo, which respectively represent the everyday closing price of China (Mainland), Hong Kong and United States in the past two years. Since different stock markets have the different opening dates, we exclude the

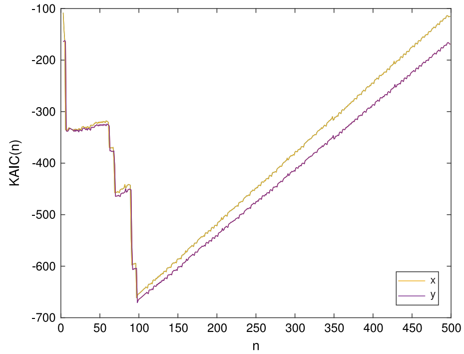

Fig. 10. Simulation of KAIC based on Lozi map.

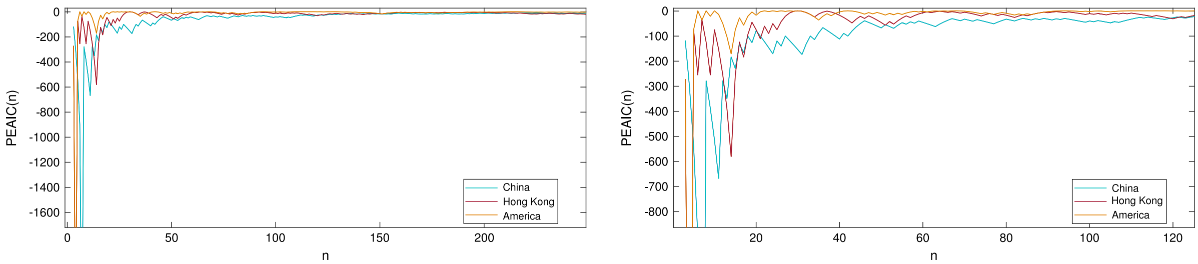

(a) PEAIC. (b) PEAIC.

Fig. 11. Numerical results of PEAIC.

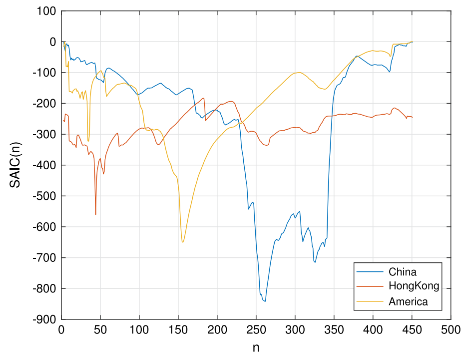

Fig. 12. Numerical results of SAIC.

asynchronous date and then relink the rest so that we can get time series of the same length. After that, we apply the AIC method to skewness, kurtosis and entropy to discuss its practical applications.

4.2. Results and discussion

We standardize the stock data, and calculate by substituting generalized AIC method which is generally denoted as $GAIC\ (n)$:

$$GAIC\ (n) = n \ln \left[\tilde{A}\,(1, n)\right] + (N - n - 1) \ln \left[\tilde{A}\,(n + 1, N)\right] \tag{19}$$

As what has been mentioned in Section 2, we obtain three generalized AIC functions, which is defined as PEAIC, SAIC and KAIC based on the three groups of stock data.

The plot is shown as follows (see Fig. 11):

Table 1
Abnormal points from the Shanghai index and events at the time point.

Deviation point of skewness	36th	185th	240th	345th	424th
Date	2017.5.17	2016.9.9	2016.6.13	2016.12.29	2015.8.21
The trend of SSEC	descend	descend	descend	ascend	ascend
The trend of HSI	descend	ascend	ascend	ascend	ascend
The trend of DJI	descend	ascend	ascend	ascend	ascend
Events	In May 18th, affected by political turmoil, the U.S. stock market, the dollar and Treasury yields all fell sharply.	(1) SONY PS4 version released on Thursday. (2) Companies related to Zika virus epidemic expected to benefit. (3) The large aircraft C919 first flew at the end of 2016, and a huge industrial chain would break out soon.	(1) The U.S. stocks fell sharply and the market panic keep rising for three months. (2) Resulting from Britain out of Europe, European shares fell more than 1% that hit three months lowest. (3) The United States oil keep falling.	Central Bank took measures to develop sound macro Prudential policy framework to prevent system risk	(1) Global stock markets slumped in Aug. 2015. (2) China's economic growth slowed, Brazil plunged into recession. (3) The Fed's interest rate hike was expected to continue.

Table 2
Outliers shown by the KAIC function.

Kurtosis mutation point	35th	55th	170th	185th	230th	324th	428th
Date	2017.5.18	2017.4.18	2016.9.29	2016.9.6	2016.6.27	2016.12.31	2016.8.17
The trend of SSEC	descend	descend	ascend	descend	ascend	ascend	descend
The trend of HSI	descend	descend	descend	ascend	descend	ascend	descend
The trend of DJI	descend	ascend	descend	descend	ascend	descend	descend
Events	U.S. stocks fell.				Brexit vote.	The SSEC got a rise of 9.4 percent for the first time in two years.	Chinese government delivered solutions to save stock market.

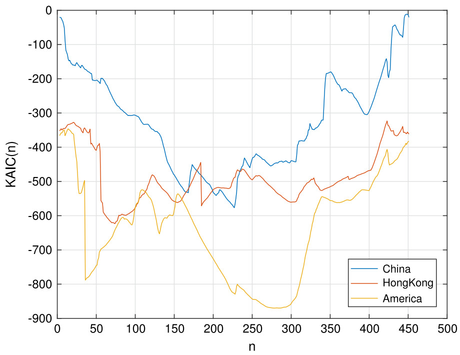

Fig. 13. Numerical results of KAIC.

The advantage of permutation entropy is that every generated value contains abundant data information. We find the volatility structure of the three sets of data is obviously different for $0 < n < 50$. The PEAIC of DJI, HSI, SSEC volatility decline successively, but the PEAIC of SSEC and HSI change more slowly, except for the initial mutation. With the increase of variable n, the all three curves tend to be stable. Applying the popularized AIC model to 3rd order moment of the three sets of indexes, some obvious anomaly points appear. The SAIC of HSI and DJI are back to normal after the chop point, while the curve of SSEC changes more slowly. We notice some abnormal points in Fig. 12 and find the events at the corresponding time point from the data.

It is summed up in Table 1.

In Fig. 13, we can find that the discrepancy of the stock markets of US, China (mainland) and Hong Kong under the perspective of higher order method. In addition, stock indexes in the different region embodies different volatility structures. The overall performance of KAIC curve of the SSEC decreases first and then increases, the curve of the HSI fluctuates in a small range, while the KAIC plot of DJI shows similar fluctuations of sine function for $50 < n < 350$. Similarly, we summarize the outliers from the curve of KAIC, which are shown in Table 2.

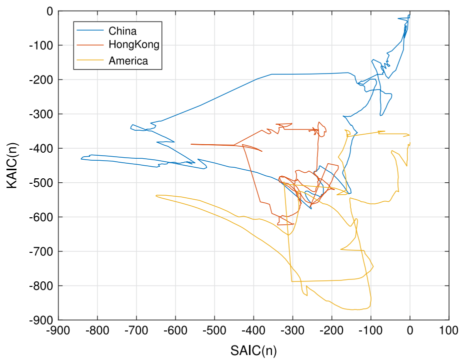

Fig. 14. Numerical results of S-KAIC.

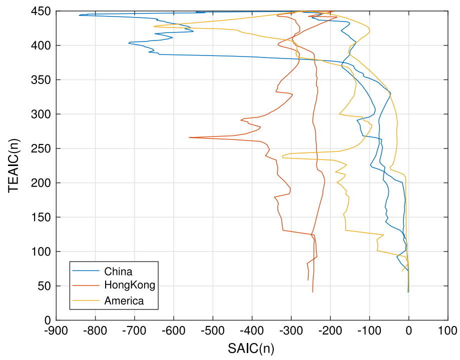

Fig. 15. Numerical results of S-TEAIC.

4.3. The relation between skewness, kurtosis and Tsallis entropy

We take the three different types of stock data of SSEC, HSI and DJI into SAIC and KAIC, and constitute the AIC plane by utilizing SAIC as x axis and KAIC as y axis, denoted as S-KAIC, so that more information could be revealed on this higher dimensional model.

As we can see from Fig. 14 , discrepancies appear in different stock markets, which represent diverse marketing environments. For the same level of skewness, the curve of SSEC, HSI and DJI decline successively, which is corresponding to the current situation of the region's economic development.

It is noteworthy that Figs. 14–16 have some similarities on the volatility structure. There is an overt mutation in the SSEC at the kurtosis of -450. The same situation occurs when the $KAIC(n)$ of HSI equals to -400, and the $KAIC(n)$ of DJI equals to -550. The volatility of Figs. 14–16 also shows the same pattern in the absolute minimum of skewness and the absolute minimum of the kurtosis. It is also intriguing that, compared to DJI, the KAIC plots of SSEC and HSI have a high similarity in volatility structure.

Higher dimensional AIC plane reflects more information of different stock market. Comparing Figs. 15 and 16, it is clear that under the effect of Tsallis Entropy, the data of the three groups have their respective fluctuation characteristics. The S-TEAIC and K-TEAIC of HSI and DJI in Fig. 15 almost have the same fluctuation structure when $0 < TEAIC(n) < 400$. But the change of HSI is relatively backward compared to the curve of DJI. In the meantime, the curve of SSEC shows a different undulation from the other two, reflecting the difference of marketing policy of three areas. It is also apparent that SAIC reflects the relationship between stock markets in different regions in a better way to some extent.

To sum up, in spite of diverse economic situation in different regions, we can see that the AIC plane of mainland, Hong Kong and the United States have a certain degree of similarity, and Hong Kong has the most constrictive fluctuation plot among the three.

5. Conclusion

To begin with, we generalized the Akaike information criterion to high-order statistics such as skewness, kurtosis and permutation entropy to analyze the volatility of financial time series.

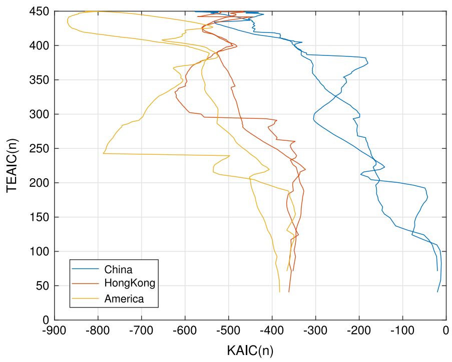

Fig. 16. Numerical results of K-TEAIC.

While variance reflects the level of volatility, skewness refers to the degree of asymmetry of frequency distribution, which is a measure of the asymmetrical distribution of the sample data, and kurtosis measures the change of the tailedness. They demonstrate volatility behaviors of time series in different aspects, which can reflect more detailed information than variance.

Moreover, a new method — AIC plane, which correlate SAIC, KAIC and Tsallis entropy, is devised to effectively demonstrate the time-dependent information. Then, by using logistic map model and lozi map model, Simulations are used on stock market data to provide comparative study of the original and modified Akaike information criterion. In the first simulation of generalized AIC method, it can be illustrated that the SAIC differs from curves of AIC in many aspects. In contrast, KAIC has a more similar going-up trend compared to AIC, but AIC is steeper and smoother for that high-order statistics can detect information that cannot be expressed by low-order statistics. But in another aspect, the SAIC roughly retains a feature of AIC, that is, the larger r is, the smaller AIC is. Nevertheless, in curves of KAIC, when $r = 3.7$ and $r = 3.8$ the curves is above those when $r = 3.9$ and 4.0. In second simulation, we can found similar results as well. What is different is that this time both SAIC and KAIC change the relative values compared to AIC.

By using generalized AIC method of skewness, kurtosis and Permutation entropy as well as the method of AIC plane we proposed heuristically, more interesting results of volatility behaviors in China(mainland), American and Hong Kong's stock markets have been unearthed. We observe the stock data from the three areas based on their volatility and make vertical and horizontal comparisons in different perspective, and conclude that there are some differences of AIC, SAIC and KAIC structures between the stock markets of China (mainland), Hong Kong and America.

Comparing the three plots of the AIC plane above, we notice that the three regions have similar tendency to some extent, but they have their own fluctuation characteristics, and the results of financial time series verify the reliability of our simulations.

In the S-KAIC plane, we can see that the volatility structures of the Hong Kong stock market data are more similar to the numerical results of mainland than United States. While in S-TEAIC plane and K-TEAIC plane, it demonstrates a volatility similarity to the US stock market rather than China (Mainland). In this case, it is obvious that the AIC plane we proposed can creatively show more fluctuation information of financial time series, which cannot be detected when using generalized AIC method solely, and it can also reflect the essential relationship of different market systems. However, there are still further researches need to be promoted to analyze financial risk, or other use of financial time series. Moreover, the practical applications such as risk analysis in financial market are yet to be mined.

Acknowledgments

The financial supports from the funds of the China National Science (61771035, 61371130) and the Beijing National Science, China (4162047) are gratefully acknowledged.

References

[1] P. Grassberger, I. Procaccia, Dimensions and entropies of strange attractors from a fluctuating dynamics approach, Physica D 13 (1–2) (1984) 34–54.
[2] H.D. Abarbanel, J.P. Gollub, Analysis of observed chaotic data, Phys. Today 49 (1996) 86.
[3] H. Xiong, P. Shang, Weighted multifractal cross-correlation analysis based on shannon entropy, Commun. Nonlinear Sci. Numer. Simul. 30 (1) (2016) 268–283.
[4] R.N. Mantegna, H.E. Stanley, Scaling behaviour in the dynamics of an economic index, Nature 376 (6535) (1995) 46–49.
[5] R.N. Mantegna, E.H. Stanley, N.A. Chriss, An introduction to econophysics: Correlations and complexity in finance, Phys. Today 53 (12) (2000) 70.
[6] F.J. DePenya, L.A. Gil-Alana, Serial correlation in the Spanish stock market, Glob. Finance J. 18 (1) (2007) 84–103.
[7] P. Grau-Carles, Empirical evidence of long-range correlations in stock returns, Physica A 287 (3) (2000) 396–404.
[8] P. Grau-Carles, Long-range power-law correlations in stock returns, Physica A 299 (3) (2001) 521–527.

[9] Y. Yin, P. Shang, Modified DFA and DCCA approach for quantifying the multiscale correlation structure of financial markets, Physica A 392 (24) (2013) 6442–6457.
[10] C. Liu, W.-X. Zhou, Superfamily classification of nonstationary time series based on DFA scaling exponents, J. Phys. A 43 (49) (2010) 495005.
[11] J. Zhi-Qiang, Z. Wei-Xing, Direct evidence for inversion formula in multifractal financial volatility measure, Chin. Phys. Lett. 26 (2) (2009) 028901.
[12] A. Lin, P. Shang, X. Zhao, The cross-correlations of stock markets based on DCCA and time-delay DCCA, Nonlinear Dynam. 67 (1) (2012) 425–435.
[13] Q. Tian, P. Shang, G. Feng, Financial time series analysis based on information categorization method, Physica A 416 (2014) 183–191.
[14] J.T. Machado, F.B. Duarte, G.M. Duarte, Analysis of stock market indices through multidimensional scaling, Commun. Nonlinear Sci. Numer. Simul. 16 (12) (2011) 4610–4618.
[15] D. Faranda, F.M.E. Pons, E. Giachino, S. Vaienti, B. Dubrulle, Early warnings indicators of financial crises via auto regressive moving average models, Commun. Nonlinear Sci. Numer. Simul. 29 (1) (2015) 233–239.
[16] X. Lu, E.R. Putri, Semi-analytic valuation of stock loans with finite maturity, Commun. Nonlinear Sci. Numer. Simul. 27 (1) (2015) 206–215.
[17] J.R.C. Piqueira, L.P.D. Mortoza, Brazilian exchange rate complexity: Financial crisis effects, Commun. Nonlinear Sci. Numer. Simul. 17 (4) (2012) 1690–1695.
[18] R.S. Tsay, Analysis of Financial Time Series, Vol. 543, John Wiley & Sons, 2005.
[19] X. Gabaix, P. Gopikrishnan, V. Plerou, H.E. Stanley, A theory of power-law distributions in financial market fluctuations, Nature 423 (6937) (2003) 267.
[20] V. Plerou, P. Gopikrishnan, H.E. Stanley, Econophysics: Two-phase behaviour of financial markets, Nature 421 (6919) (2003) 130–130.
[21] T. Lux, M. Marchesi, Scaling and criticality in a stochastic multi-agent model of a financial market, Nature 397 (6719) (1999) 498.
[22] K.J. Forbes, R. Rigobon, No contagion, only interdependence: Measuring stock market comovements, J. Finance 57 (5) (2002) 2223–2261.
[23] T. Lux, M. Marchesi, Volatility clustering in financial markets: A microsimulation of interacting agents, Int. J. Theor. Appl. Finance 3 (04) (2000) 675–702.
[24] V. Plerou, P. Gopikrishnan, L.A.N. Amaral, M. Meyer, H.E. Stanley, Scaling of the distribution of price fluctuations of individual companies, Phys. Rev. E 60 (6) (1999) 6519.
[25] R. Albert, A.-L. Barabási, Statistical mechanics of complex networks, Rev. Modern Phys. 74 (1) (2002) 47.
[26] D.-M. Song, M. Tumminello, W.-X. Zhou, R.N. Mantegna, Evolution of worldwide stock markets, correlation structure, and correlation-based graphs, Phys. Rev. E 84 (2) (2011) 026108.
[27] R.N. Mantegna, Hierarchical structure in financial markets, Eur. Phys. J. B 11 (1) (1999) 193–197.
[28] J.-P. Onnela, K. Kaski, J. Kertész, Clustering and information in correlation based financial networks, Eur. Phys. J. B 38 (2) (2004) 353–362.
[29] V. Boginski, S. Butenko, P.M. Pardalos, Statistical analysis of financial networks, Comput. Statist. Data Anal. 48 (2) (2005) 431–443.
[30] C. Stărică, C. Granger, Nonstationarities in stock returns, Rev. Econom. Stat. 87 (3) (2005) 503–522.
[31] L. Laloux, P. Cizeau, J.-P. Bouchaud, M. Potters, Noise dressing of financial correlation matrices, Phys. Rev. Lett. 83 (7) (1999) 1467.
[32] T. Di Matteo, T. Aste, M.M. Dacorogna, Long-term memories of developed and emerging markets: Using the scaling analysis to characterize their stage of development, J. Bank. Finance 29 (4) (2005) 827–851.
[33] G. Kitagawa, H. Akaike, A procedure for the modeling of non-stationary time series, Ann. Inst. Statist. Math. 30 (1) (1978) 351–363.
[34] Y. Teng, P. Shang, Detrended fluctuation analysis based on higher-order moments of financial time series, Physica A 490 (2018) 311–322.
[35] K. Manomaiphiboon, S.-K. Park, A.G. Russell, Accounting for high-order correlations in probabilistic characterization of environmental variables, and evaluation, Stoch. Environ. Res. Risk Assess. 22 (2) (2008) 159–168.
[36] C.N. Haas, On modeling correlated random variables in risk assessment, Risk Anal. 19 (6) (1999) 1205–1214.
[37] S. Saleh, Robust AIC with high breakdown scale estimate, J. Appl. Math. 2014 (2014) 241–249.
[38] Y. Fujikoshi, R. Enomoto, T. Sakurai, High-dimensional in the growth curve model, J. Multivariate Anal. 122 (2013) 239–250.
[39] T. Sakurai, T. Nakada, Y. Fujikoshi, High-dimensional aics for selection of variables in discriminant analysis, Sankhya A 75 (1) (2013) 1–25.
[40] H. Ogasawara, Bias correction of the akaike information criterion in factor analysis, J. Multivariate Anal. 149 (2016) 144–159.
[41] P. Wagenaars, P. Wouters, P. van der Wielen, E. Steennis, Accurate estimation of the time-of-arrival of partial discharge pulses in cable systems in service, IEEE Trans. Dielectr. Electr. Insul. 15 (4) (2008) 1191.
[42] J.H. Kurz, C.U. Grosse, H.-W. Reinhardt, Strategies for reliable automatic onset time picking of acoustic emissions and of ultrasound signals in concrete, Ultrasonics 43 (7) (2005) 538–546.
[43] H. Zhang, C. Thurber, C. Rowe, Automatic P-wave arrival detection and picking with multiscale wavelet analysis for single-component recordings, Bull. Seismol. Soc. Am. 93 (5) (2003) 1904–1912.
[44] P.K. Sahoo, G. Arora, A thresholding method based on two-dimensional Renyi's entropy, Pattern Recognit. 37 (6) (2004) 1149–1161.
[45] C. Bandt, B. Pompe, Permutation entropy: A natural complexity measure for time series, Phys. Rev. Lett. 88 (17) (2002) 174102.
[46] B. Fadlallah, B. Chen, A. Keil, J. Príncipe, Weighted-permutation entropy: A complexity measure for time series incorporating amplitude information, Phys. Rev. E 87 (2) (2013) 022911.
[47] M. Xu, P. Shang, J. Huang, Modified generalized sample entropy and surrogate data analysis for stock markets, Commun. Nonlinear Sci. Numer. Simul. 35 (2016) 17–24.
[48] T. Schreiber, Measuring information transfer, Phys. Rev. Lett. 85 (2) (2000) 461.
[49] J.S. Richman, J.R. Moorman, Physiological time-series analysis using approximate entropy and sample entropy, Am. J. Physiol.-Heart Circ. Physiol. 278 (6) (2000) H2039–H2049.
[50] É. Roldán, J.M. Parrondo, Entropy production and Kullback-Leibler divergence between stationary trajectories of discrete systems, Phys. Rev. E 85 (3) (2012) 031129.
[51] Y. Li, X.-p. Fan, G. Li, New image threshold segmentation algorithm, Minimico Systems-Shenyang 27 (11) (2006) 2125.
[52] L. Lacasa, A. Nunez, É. Roldán, J.M. Parrondo, B. Luque, Time series irreversibility: A visibility graph approach, Eur. Phys. J. B 85 (6) (2012) 217.
[53] R. Sleeman, T. Van Eck, Robust automatic P-phase picking: An on-line implementation in the analysis of broadband seismogram recordings, Phys. Earth Planet. Interiors 113 (1–4) (1999) 265–275.
[54] M. Leonard, B. Kennett, Multi-component autoregressive techniques for the analysis of seismograms, Phys. Earth Planet. Interiors 113 (1–4) (1999) 247–263.
[55] N. Maeda, A method for reading and checking phase times in auto-processing system of seismic wave data, Zisin 38 (3) (1985) 365–379.
[56] M. Leonard, Comparison of manual and automatic onset time picking, Bull. Seismol. Soc. Am. 90 (6) (2000) 1384–1390.